On-chip optical true time delay lines featuring one-dimensional fishbone photonic crystal waveguide

Chi-Jui Chung, Xiaochuan Xu, Gencheng Wang, Zeyu Pan, and Ray T. Chen

Citation: Appl. Phys. Lett. **112**, 071104 (2018);
View online: https://doi.org/10.1063/1.5006188
View Table of Contents: http://aip.scitation.org/toc/apl/112/7
Published by the American Institute of Physics

On-chip optical true time delay lines featuring one-dimensional fishbone photonic crystal waveguide

Chi-Jui Chung,[1,a),b)] Xiaochuan Xu,[2,a)] Gencheng Wang,[1,c)] Zeyu Pan,[1] and Ray T. Chen[1,2,b)]
[1]*Microelectronic Research Center, Department of Electrical and Computer Engineering, The University of Texas at Austin, Austin, Texas 78758, USA*
[2]*Omega Optics, Inc., Austin, Texas 78757, USA*

(Received 22 September 2017; accepted 28 December 2017; published online 14 February 2018)

In this paper, we present on-chip optical true time delay lines based on slow light one-dimensional (1D) fishbone photonic crystal waveguides (FPCWs). The structural slow light is generated by modulating the index guided optical mode with periodically arranged sidewalls along the propagation direction. Due to the reduced mode overlap with the rough etched surface, the propagation loss of the 1D FPCW is significantly reduced compared to the two-dimensional photonic crystal waveguide. A delay time of 65 ps/mm is observed experimentally. *Published by AIP Publishing.*
https://doi.org/10.1063/1.5006188

Microwave signal processing and transmission demand large bandwidth time delays. However, conventional electrical phase shifters intrinsically have a narrow bandwidth, which significantly deteriorates the performance of microwave systems. For example, phased array antenna (PAA)[1] is an intriguing technology for high performance communication and radar systems for both civilian[2] and military applications[3] because of the high directivity and fast steering capability. The array is composed of multiple sets of antenna units with their own phase shifters. The signal from the transmitter is fed into each phase shifter. Through tuning the phase difference between each antenna unit, beams of radio waves in the desired frequency range are formed to point into a desired direction. However, due to the narrow bandwidth of electrical phase shifters and thus the induced beam squint effect, the bandwidth of the PAA system is extremely narrow.

An optical true time delay line (OTTDL) is a promising alternative as its bandwidth is intrinsically large. Numerous OTTDL designs have been studied so far, including bulk optics,[4] dispersive fiber,[5] and acoustic-optic integrated circuits.[6] These photonic solutions consist of discrete or low dispersion optical components and therefore are bulky in size and have stringent alignment requirements. Recently, various on-chip OTTDL structures have been investigated to realize ultra-compact and robust true time delay (TTD) lines such as photonic crystal waveguides (PCWs),[7–10] polymer waveguides,[11] and graphene based waveguides.[12] Among these structures, due to the strong optical confinement[13] and slow-light effect,[14] silicon PCW TTD lines can significantly reduce the footprint and power consumption. In addition, leveraging the matured CMOS fabrication, the cost of silicon PCW photonic chips can be greatly reduced. Due to the less etched surface area overlapped with the optical mode compared to two-dimensional (2D) PCW, slow light silicon one-dimensional (1D) fishbone photonic crystal waveguides (FPCWs) have been experimentally demonstrated with lower optical propagation loss and less susceptibility to fabrication variations.[15] Furthermore, the light confinement of 1D FPCW relies on index confinement. Thus, its footprint could be reduced compared to 2D PCW and therefore is more appealing for high density integration of TTD lines.[15] In this paper, we experimentally demonstrated an on-chip wavelength tunable OTTDL featuring 1D FPCWs. The demonstrated TTD module provides compact footprint, low loss, and large time delay. It can potentially be used in microwave applications such as multi-frequency PAAs.

Figure 1(a) illustrates the schematic of the 1D FPCW. The structural slow light is generated by periodically modulated sidewalls along the propagation direction, and the light is confined in the vertical directions through index guiding. Since laterally odd modes are difficult to excite with a monomode strip waveguide, we will focus on laterally even modes, which are also referred to as quasi-transverse electrical (quasi-TE) modes. The band diagram of even modes in the 1D FPCW is shown in Fig. 1(b). The light cone regions represent modes that extend into the top or bottom claddings. Incomplete bandgaps exist between bands 1 and 2, as well as bands 2 and 3, as illustrated by the green regions in Fig. 1(b). The mode profiles ($|Ez|^2$) of the modes are shown in Figs. 1(c)–1(h). The corresponding group index is plotted in Fig. 1(i). Eminent slow light phenomena are observed close to the edge of the Brillouin zone. In band 0, as $a/\lambda \ll 1$, the periodic corrugation can be considered as a uniform material according to effective medium theory except the region near the band edge, where $a/\lambda \sim 0.216$. The slow light bandwidth is very narrow and thus not suitable for TTDs due to the power penalty induced by large group velocity dispersion (GVD). Bands 1 and 2 have a larger slow light bandwidth due to the anti-crossing effect. Slow light occurs not only near the band edge but also near the anti-crossing point. However, there exist two modes, as shown in Fig. 1(i), making it difficult to selectively couple into one of the modes. Thus, we concentrate on band 2.

[a)]C.-J. Chung and X. Xu contributed equally to this work.
[b)]Electronic addresses: cjchung@utexas.edu and chen@ece.utexas.edu
[c)]Present address: College of Information Science and Electronic Engineering and the Cyrus Tang Center for Sensor Materials and Applications, Zhejiang University, Hangzhou 310027, China.

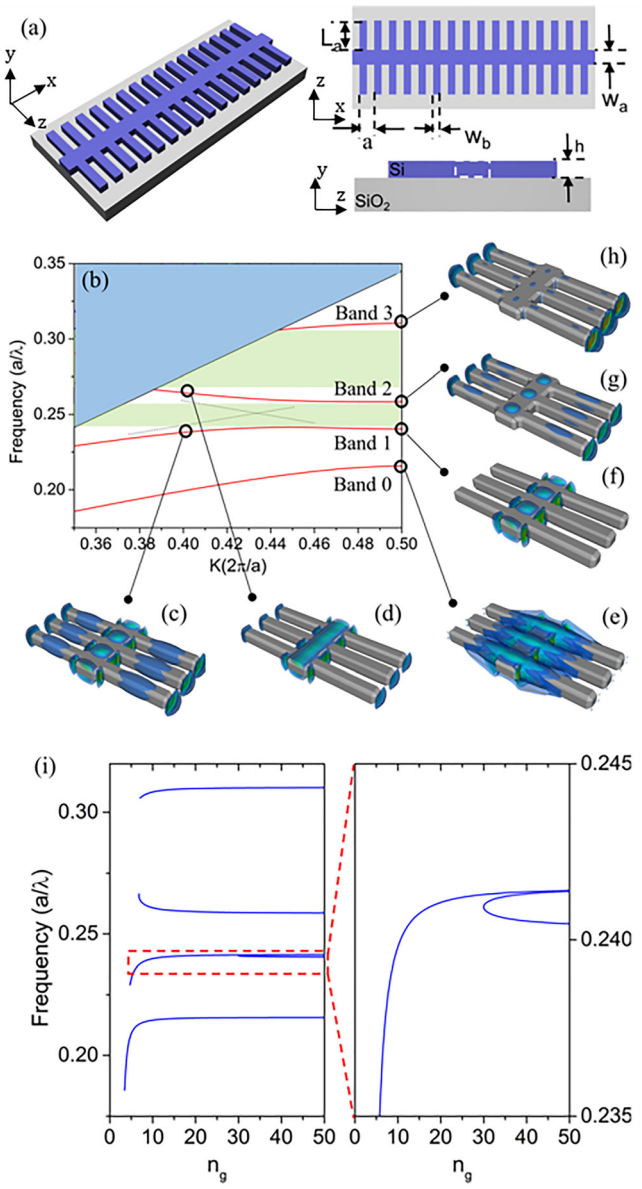

FIG. 1. (a) Schematic of the proposed 1D FPCW structure. (b) Band diagram of the 1D FPCW. (c)–(h) Ez distributions of the modes in bands 0–3. (i) Group indices of the bands.

The 1D FPCW structure is optimized using the 3D plane wave expansion method targeting at generating large time delay with a compact footprint. As shown in Fig. 2, the period (a), tooth width (Wb), tooth length (La), and center strip width (Wa) are optimized to be 400 nm, 188 nm, 1000 nm, and 400 nm, respectively, and the structure is designed to be built on a silicon-on-insulator (SOI) wafer with a 220 nm thick device silicon layer and a 3 μm thick buried oxide (BOX) layer. This proposed structure also benefits from lateral index guiding instead of bandgap guiding in 2D PCW. Therefore, the waveguide width is only 2.4 μm, which is 62% size reduction compared to 2D PCW.[14] The simulation results prove the slow light effect with a minimum group index of 6.3 and strong GVD around -1.5×10^7 ps/(nm km), as shown in Fig. 2(a). A delay time of 50 ps can be easily achieved with 1 mm 1D FPCW through tuning the wavelength between 1530 nm and 1565 nm where the group index is greater than 15. In order to reduce the strong reflection at the interface between the strip waveguide and 1D FPCW, step tapers[16] comprising four periods are designed. As shown in Fig. 2(b), the coupling efficiency is greatly increased to 72%.

The device fabrication starts with the SOI wafer with a 250 nm silicon device layer (SOITEC). The silicon device layer is thinned down to 230 nm through multiple cycles of thermal oxidation and wet etching. A silicon dioxide hard mask is formed by further oxidizing 10 nm silicon, leaving a 220 nm silicon device layer. The waveguides are patterned using a Jeol FSE 6000 e-beam lithography system and reactive ion etching (RIE). The scanning electron microscopy (SEM) images of the fabricated 1D FPCW are shown in Fig. 3(a). Subwavelength grating couplers are utilized to couple light in and out of the on-chip circuit, the SEM image of which is shown in Fig. 3(b).[17,18]

The transmission spectrum of a 500 μm long 1D FPCW with tapers is shown in Fig. 4(a). It is obtained using a Thorlab ASE-FL7001P broadband amplified spontaneous emission (ASE) source with a TE polarizer covering 1530–1610 nm and an optical spectrum analyzer (OSA). The transmission spectrum shows the lowest optical loss of 3.729 dB at 1565.14 nm which is observed for the 500 μm long 1D FPCW with tapers. The group index of the 1D FPCW is derived using the interference pattern on the spectrum of an unbalanced testing Mach-Zehnder interferometer (MZI) fabricated on the same chip with one arm of a 500 μm long 1D FPCW and the other arm of a 500 μm long and 500 nm wide silicon single mode strip waveguide. The transmission spectrum of the MZI structure is measured and shown in Fig. 4(b). Due to the group velocity difference between the two arms and the corresponding optical path difference, the interference pattern is observed on the spectrum. As the group velocity of the 1D FPCW increases at the bandgap, the period of the interference pattern becomes smaller. The relation of the group indices of the two arms can be described by[19]

$$n_{g,PCW} = n_{g,ref} + \frac{\lambda_{min} \times \lambda_{max}}{2 \times L(\lambda_{min} - \lambda_{max})}, \quad (1)$$

where $n_{g,pcw}$ is the group index of the arm with 1D FPCW and $n_{g,ref} = 4.2$ is the group index of the silicon strip reference waveguide. $L = 500$ μm is the physical length of the 1D FPCW. λ_{max} and λ_{min} are the wavelength at local power maxima and minima of the spectrum, respectively. As shown in Fig. 4(b), the highest group index observed is 31.6 and the lowest is 6.55. Although there is a ~25 nm red shift of the transmission spectrum and a slow light wavelength region compared to simulation results due to the fabrication error, the trend closely matches the simulation.

To measure the propagation loss and time delay of the proposed 1D FPCW, four TTD lines are fabricated. As shown in Fig. 5(a), the device uses grating couplers for efficient coupling and two cascaded 1 × 2 Y-junction splitters to fan out into four waveguides with different 1D FPCW lengths. From the top to bottom, waveguide channel-1 to channel-4 contain 3 mm, 2 mm, 1 mm, and 0 mm silicon single mode strip waveguides and 0 mm, 1 mm, 2 mm, and 3 mm 1D FPCW, respectively. The transmission spectra of channels-2, 3, and 4 are measured and normalized to those of channel-1 (strip waveguide), and the propagation loss of the

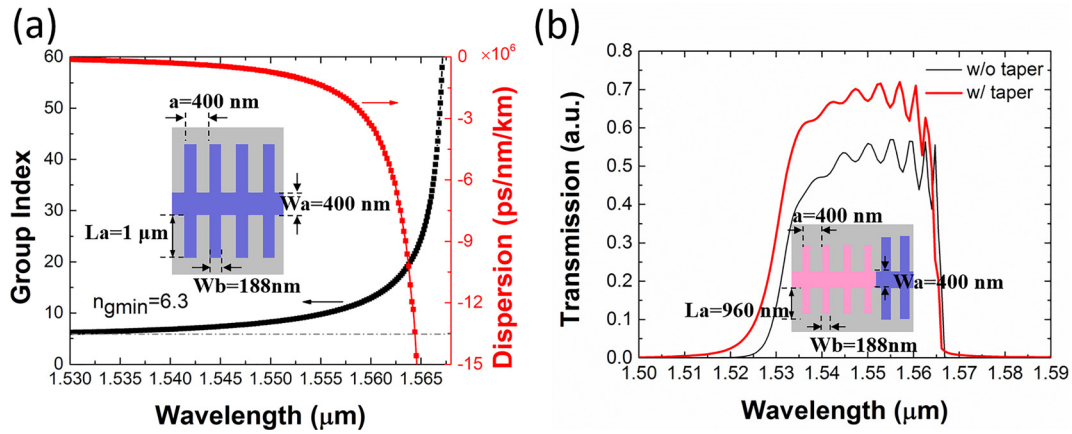

FIG. 2. (a) Group index and dispersion of band 2 when a = 400 nm, Wb = 188 nm, La = 1000 nm, and Wa = 400 nm. Black: Group index. Red: Dispersion. (b) Simulated transmission curve. Black: Without the step taper. Red: With the step taper.

1D FPCWs is measured using the cut-back method with the same four-channel TTD module. The photonic band edge shifts from 1591.6 nm of the testing waveguides to 1579.55 nm, due to the fabrication error and wafer thickness variations. By comparing the transmission spectra of the four channels with different 1D FPCW lengths and fitting the length dependence, the propagation loss of 1D FPCW versus wavelength plot can be achieved as shown in Fig. 5(b). The lowest propagation loss is 0.79 dB/mm at 1563.87 nm, and the propagation loss at the edge of the bandgap at 1579 nm is 2.84 dB/mm.

In the time delay measurement, channel-1 (with a 3 mm silicon strip waveguide) is chosen as the reference waveguide. Time delays of channel-2 to channel-4 are measured with regard to the reference waveguide. The delay of the reference waveguide is calculated and added to the time delays of channel-2 to channel 4 to get the absolute time delay generated in each channel.

The schematic of the delay time measurement setup is shown in Fig. 6(a). A 10 dBm 10–12 GHz RF signal from port 1 of the HP8510C vector network analyzer (VNA) is fed into the CODEON Mach-40 lithium niobate electro-optic

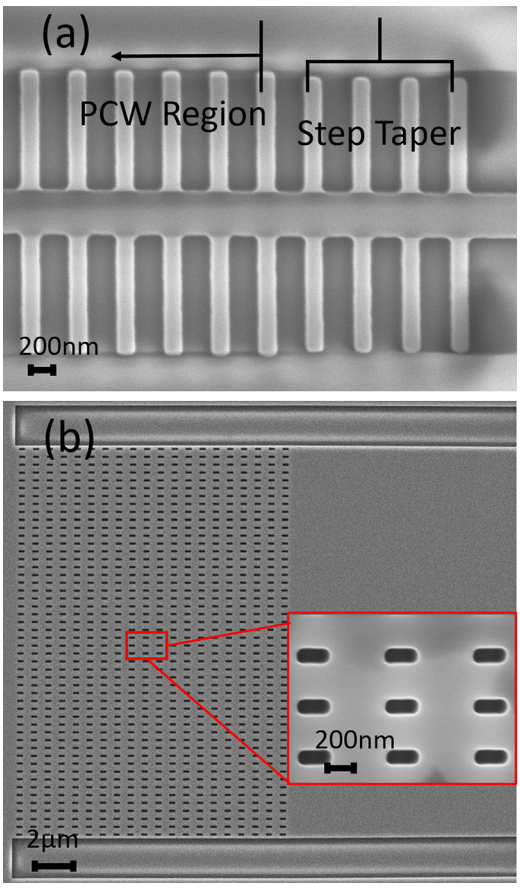

FIG. 3. SEM images of (a) 1D FPCW with the step taper (b) Subwavelength grating coupler.

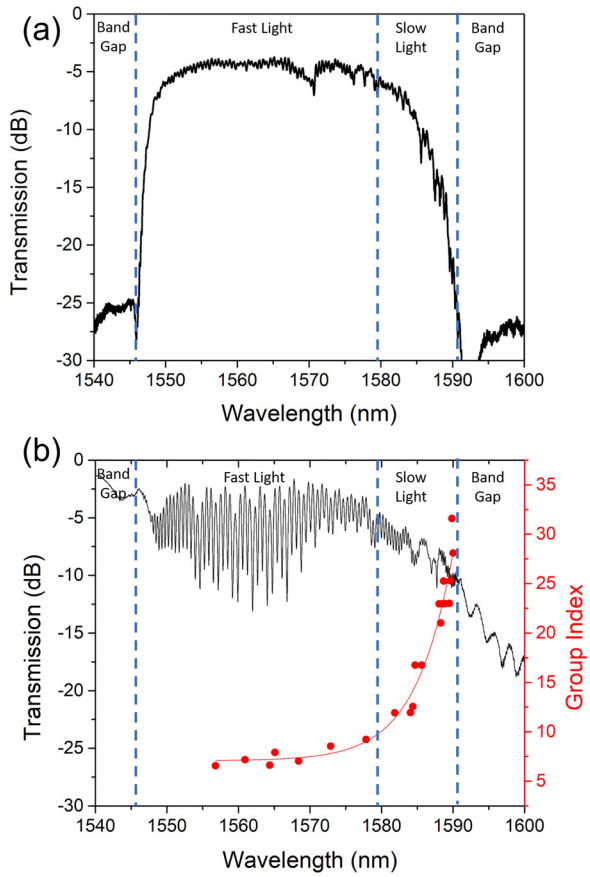

FIG. 4. (a) Transmission spectrum of a testing 500 μm long 1D FPCW. (b) Measured MZI transmission spectrum and derived group index of a 500 μm long 1D FPCW.

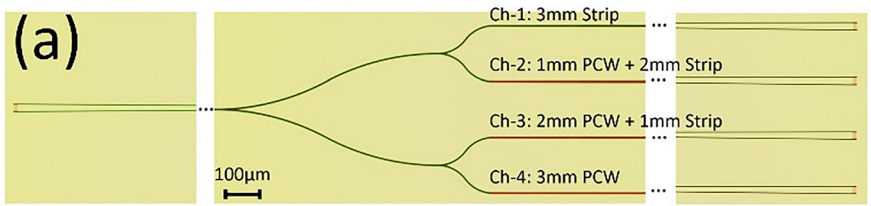

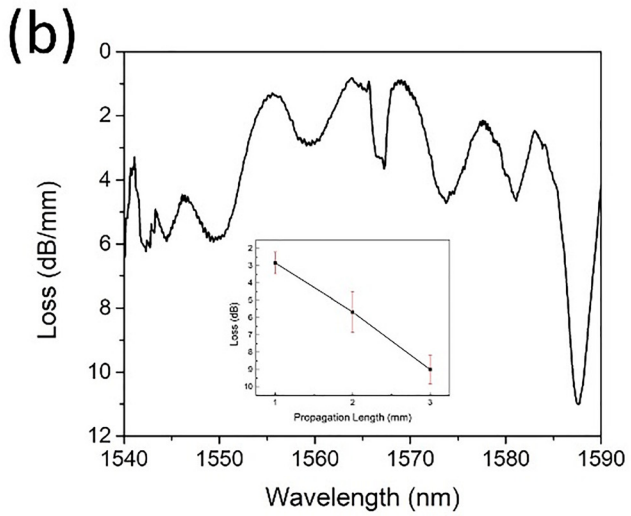

FIG. 5. (a) Optical microscopy images of the four-channel device. (b) 1D FPCW loss spectrum derived from the cut-back method from waveguides with different 1D FPCW lengths. The inset shows the measured transmission versus propagation length plot at 1579 nm.

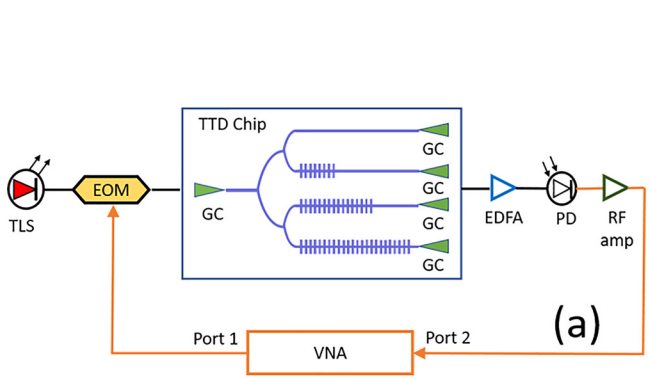

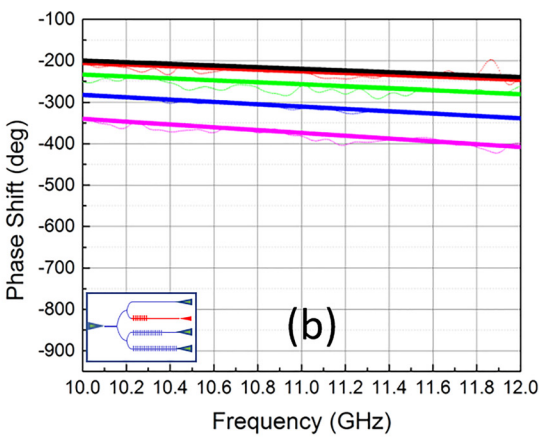

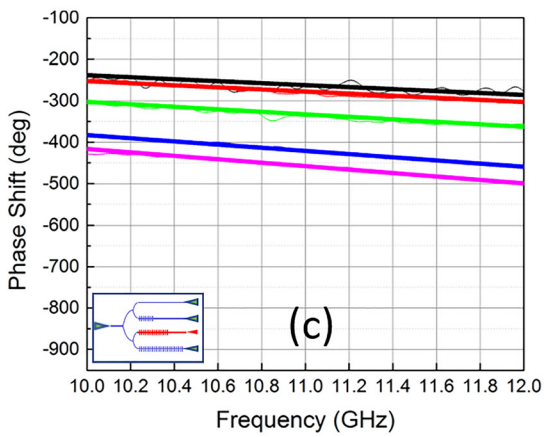

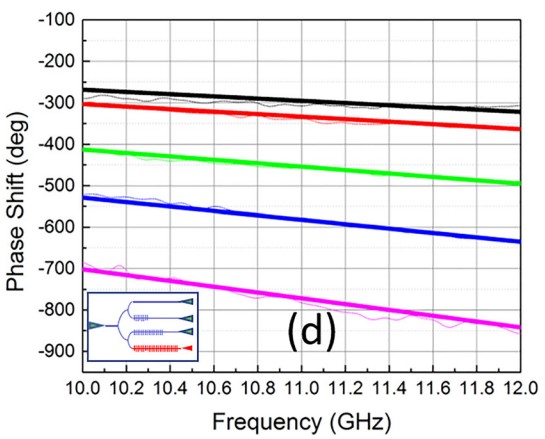

FIG. 6. (a) Wavelength continuously tunable time delay measurement setup for 1D FPCW TTD lines. TLS: Tunable laser source; GC: Grating couplers; and Phase-frequency curves for (b) Channel-2 (1 mm 1D FPCW with the 2 mm silicon strip waveguide), (c) Channel-3 (2 mm 1D FPCW with the 1 mm silicon strip waveguide), and (d) Channel-4 (3 mm 1D FPCW). From top to bottom, each color line represents the measurements at $\lambda = 1567$ nm (black), 1570 nm (red), 1573 nm (green), 1576 nm (blue), and 1579 nm (magenta) respectively.

(EO) modulator to modulate the light from a tunable laser. The modulated light is then coupled into the four-channel module. A JDS Uniphase L-band erbium doped fiber amplifier (EDFA) is added to increase the signal to noise ratio. The optical signal is converted back into the RF electrical signal (New Focus 1014 high speed photodiode), amplified, and then fed back to VNA port 2. The delay time of the TTD module is derived from the phase versus frequency relation of the S_{21} parameter.

Due to the coverage of the L-band EDFA, the four channel TTD module is tested from 1567 nm to 1579 nm with a 3 nm step because 1567 nm is the shortest wavelength the L-band EDFA can cover. The phase-frequency curves are shown in Figs. 6(b)–6(d). The time delay (τ) generated by slow light PCW is derived from a linear regression fit of the data points using the following equation:

$$\tau = \frac{\Delta\phi}{\Delta\omega}, \tag{2}$$

where $\Delta\phi$ is the phase change over the measured frequency range $\Delta\omega$. It is a confirmation of true time delay without the beam squint effect.[14] Since the group index increases with the wavelength and therefore the time delay rises, the slope of the phase curves decreases with wavelength. High linearity of the phase-frequency relation can be seen in the three channels, which proves the beam-squint free property of OTTDL.

From Figs. 6(b)–6(d), the largest delay occurs at 1579 nm. The time delays for Channel-2 (2 mm silicon strip waveguide with 1 mm 1D FPCW), Channel-3 (1 mm silicon strip waveguide with 2 mm 1D FPCW), and Channel-4 (3 mm 1D FPCW) are 94.43 ps, 115.63 ps, and 194.9 ps. The maximum time delay we measured for 3 mm 1D FPCW is 194.9 ps which corresponds to a group index of 19.47.

In conclusion, we have proposed, fabricated, and demonstrated an on-chip four-channel optical TTD module based on 1D FPCWs. The 1D FPCW shows a low loss, strong slow light effect, and high dispersion and therefore is ideal for ultra-compact and low power consumption applications. The on-chip TTD module offers continuous tunability up to 194.9 ps and the lowest optical propagation loss of 0.79 dB/mm. Further delay can be achieved by increasing the length of the 1D FPCW region.

The authors would like to acknowledge the Air Force Office of Scientific Research (AFOSR) for supporting this work under Small Business Innovation Research (SBIR) (Contract #: FA9550-C-16-0033).

[1]R. C. Hansen, *Phased Array Antennas* (John Wiley & Sons, 2009), Vol. 213.
[2]L. C. Godara, "Application of antenna arrays to mobile communications. II. Beam-forming and direction-of-arrival considerations," Proc. IEEE **85**, 1195–1245 (1997).
[3]R. DeSalvo, C. Middleton, E. Grafer, A. Cramer, K. Anzalone, E. Soto, and B. Devenport, "The convergence of microwave photonic and optical wireless systems with military communication and sensor systems," in *2016 IEEE Avionics and Vehicle Fiber-Optics and Photonics Conference (AVFOP)* (2016), pp. 191–192.
[4]X. S. Yao and L. Maleki, "A novel 2-D programmable photonic time-delay device for millimeter-wave signal processing applications," IEEE Photonics Technol. Lett. **6**, 1463–1465 (1994).
[5]H. Subbaraman, M. Y. Chen, and R. T. Chen, "Photonic dual RF beam reception of an X band phased array antenna using a photonic crystal fiber-based true-time-delay beamformer," Appl. Opt. **47**, 6448–6452 (2008).
[6]L. H. Gesell, R. E. Feinleib, J. L. Lafuse, and T. M. Turpin, "Acousto-optic control of time delays for array beam steering," Proc. SPIE **2155**, 194–204 (1994).
[7]M. L. Povinelli, S. G. Johnson, and J. D. Joannopoulos, "Tunable time delays in photonic-crystal waveguides," Proc. SPIE **6128**, 61280R (2006).
[8]F. Ohman, K. Yvind, and J. Mork, "Slow light in a semiconductor waveguide for true-time delay applications in microwave photonics," IEEE Photonics Technol. Lett. **19**(15), 1145–1147 (2007).
[9]A. Melloni, A. Canciamilla, C. Ferrari, F. Morichetti, L. O. Faolain, T. F. Krauss, R. De La Rue, A. Samarelli, and M. Sorel, "Tunable delay lines in silicon photonics: Coupled resonators and photonic crystals, a comparison," IEEE Photonics J. **2**, 181–194 (2010).
[10]M. L. Povinelli, S. G. Johnson, and J. D. Joannopoulos, "Slow-light, band-edge waveguides for tunable time delays," Opt. Express **13**(18), 7145–7159 (2005).
[11]X. Wang, B. Howley, M. Y. Chen, and R. T. Chen, "Phase error corrected 4-bit true time delay module using a cascaded 2 × 2 polymer waveguide switch array," Appl. Opt. **46**, 379–383 (2007).
[12]T. Tatoli, D. Conteduca, F. Dell'Olio, C. Ciminelli, and M. N. Armenise, "Graphene-based fine-tunable optical delay line for optical beamforming in phased-array antennas," Appl. Opt. **55**, 4342–4349 (2016).
[13]S.-i. Inoue and A. Otomo, "Electro-optic polymer/silicon hybrid slow light modulator based on one-dimensional photonic crystal waveguides," Appl. Phys. Lett. **103**, 171101 (2013).
[14]C.-Y. Lin, H. Subbaraman, A. Hosseini, A. X. Wang, L. Zhu, and R. T. Chen, "Silicon nanomembrane based photonic crystal waveguide array for wavelength-tunable true-time-delay lines," Appl. Phys. Lett. **101**, 051101 (2012).
[15]H. Yan, X. Xu, C.-J. Chung, H. Subbaraman, Z. Pan, S. Chakravarty, and R. T. Chen, "One-dimensional photonic crystal slot waveguide for silicon-organic hybrid electro-optic modulators," Opt. Lett. **41**, 5466–5469 (2016).
[16]A. Hosseini, X. Xu, D. N. Kwong, H. Subbaraman, W. Jiang, and R. T. Chen, "On the role of evanescent modes and group index tapering in slow light photonic crystal waveguide coupling efficiency," Appl. Phys. Lett. **98**(3), 031107 (2011).
[17]X. Xu, H. Subbaraman, J. Covey, D. Kwong, A. Hosseini, and R. T. Chen, "Colorless grating couplers realized by interleaving dispersion engineered subwavelength structures," Opt. Lett. **38**, 3588–3591 (2013).
[18]X. Xu, H. Subbaraman, J. Covey, D. Kwong, A. Hosseini, and R. T. Chen, "Complementary metal–oxide–semiconductor compatible high efficiency subwavelength grating couplers for silicon integrated photonics," Appl. Phys. Lett. **101**, 031109 (2012).
[19]Y. A. Vlasov, M. O'Boyle, H. F. Hamann, and S. J. McNab, "Active control of slow light on a chip with photonic crystal waveguides," Nature **438**, 65–69 (2005).